Wind and Structures, Vol. 8, No. 3 (2005) 147-161

DOI: http://dx.doi.org/10.12989/was.2005.8.3.147

Experimental study on wind-induced dynamic interference effects between two tall buildings

Peng Huang† and Ming Gu‡

State Key Laboratory for Disaster Reduction in Civil Engineering, Tongji University, Shanghai 20092, P. R. China

(Received July 30, 2003, Accepted January 20, 2005)

Abstract. Two identical tall building models with square cross-sections are experimentally studied in a wind tunnel with high-frequency-force-balance (HFFB) technique to investigate the interference effects on wind loads and dynamic responses of the interfered building. Another wind tunnel test, in which the interfered model is an aeroelastic one, is also carried out to further study the interference effects. The results from the two kinds of tests are compared with each other. Then the influences of turbulence in oncoming wind on dynamic interference factors are analyzed. At last the artificial neural networks method is used to deal with the experimental data and the along-wind and across-wind dynamic interference factor (IF_{dx} & IF_{dy}) contour maps are obtained, which could be used as references for wind load codes of buildings.

Keywords: tall building; aerodynamic interference; HFFB technique; aeroelastic model; neural networks.

1. Introduction

With the application of new materials and advanced technologies, modern tall buildings are becoming lighter and more slender than their predecessors, thus they are more sensitive to wind excitation. In addition, along with the development of modern cities, a large number of tall buildings may be constructed in a small zone. As the aerodynamic interference effects of neighboring buildings, wind loads and dynamic responses of tall buildings are usually considerably different from those of an isolated building. The interference effects on wind loads and responses of two tall buildings depend mainly on their relative location, building geometries, upstream terrain, wind directions and reduced wind velocities, etc.

Wind-induced interference effects on tall buildings have got more and more attention since 1980s (Kwok 1995, Khanduri, *et al*. 1998 and Thepmongkorn, *et al*. 2002). By far most of the researchers focused their attentions on the interference effects between two identical buildings with square cross-sections (Khanduri 2000, Thoroddsen, *et al*. 1985, Sakamoto, *et al*. 1987, Taniike 1992, Saunders and Melbourne 1980, Blessmann 1985, Bailey and Kwok 1985, Kwok 1989, Kareem 1987, Taniike and Inaoka 1988, Taniike 1991). In these studies, the researchers applied different experimental techniques to study the dynamic interference effects. Khanduri (2000) researched the interference effects on the fluctuating loads with the pressure measurements on the rigid building

† Assistant Professor, E-mail: huangtju@mail.tongji.edu.cn
‡ Professor, Corresponding Author, Tel. and Fax: +86-21-65981210, E-mail: minggu@mail.tongji.edu.cn

model, while Thoroddsen, *et al*. (1985), Sakamoto, *et al*. (1987) and Taniike (1992) used the force balance technique to measure the fluctuating base moments on the "principal" building, which is interfered by adjacent buildings. The others Saunders and Melbourne (1980), Blessmann (1985), Bailey and Kwok (1985), Kwok (1989), Kareem (1987), Taniike and Inaoka (1988) and Taniike (1991) adopted the aeroelastic model technique to measure dynamic responses of the principal building.

In fact, the model-force-balance system in a force balance test is a dynamic one. The principal model's fluctuating base moment measured in the force balance test includes the background component of the dynamic response of the building, excluding of the resonant component of the dynamic response. While in an aeroelastic model test, dynamic responses of the principal model include both the background and resonant components. The interference factors normally vary with the wind velocity and the dynamic characteristics of the principal building, thus interference effects on dynamic responses should take account of the influence of the resonant component. If the base moments (RMS value) of the principal model measured in the force balance test are directly used to calculate the interference factors, the interference factors are mainly contributed by the background component of the dynamic responses, and the influence of the resonant component will not be reflected in the results.

In view of the fact discussed above, the HFFB technique is first applied in this paper to measure the along-wind and across-wind base moments (which are used to estimate the first mode generalized loads) of the principal model interfered by another same square building model. Then the dynamic displacements at the top of the principal model with and without interference are calculated out according to the random vibration theory, which are used subsequently to calculate the dynamic interference factors. Moreover, the aeroelastic model technique is also applied to study the dynamic interference effects between the same two buildings as those in the HFFB test. The results from the two kinds of tests can support and verify each other. After that the influences of turbulence in the oncoming flow on the dynamic interference effects are analyzed. At last the artificial neural networks method is applied to deal with the experimental data and the along-wind and across-wind dynamic interference factor (IF_{dx} and IF_{dy}) contour maps are obtained.

2. Experimental arrangement

2.1. High-frequency-force-balance system

The measurement of the wind force is carried out through the use of a 5-component (F_x, F_y, M_z, M_x and M_y) dynamic balance which is installed at the bottom of the test model. The force balance system is developed by the State Key Laboratory for Disaster Reduction in Civil Engineering, Tongji University. Five strain-gauge transducers are used in the balance system, whose output signals are amplified and filtered first, then transmitted to a micro-computer. The technical specifications of the HFFB system used in this test are listed in Table 1.

Table 1 Specifications of the force balance system

Component	Full scale range	Accuracy
F_x, F_y	30 N	±0.5%
M_z	1.5 N×m	±0.5%
M_x, M_y	15 N×m	±0.5%

A 0.1 m(b)×0.1 m(b)×0.6 m(h) square cross-section building model is used as the principal model in the HFFB test. The principal model must be very light and rigid so that the natural frequency of the balance-model system is high enough to ensure that the system has essentially flat frequency response over the range of interest. The natural frequencies of overturning moments (M_x, M_y) of the balance-model system are both above 80 Hz. To reduce the influence of high frequency response of the balance-model system and environmental noise, five low-pass filters are used, whose cut-off frequencies are all set as 35 Hz. A single "interfering" building model located at different positions provides interference.

The length scale (C_l) of 1/400 is adopted, so the prototype building is 240 meters high and 40 meters wide. The wind velocity scale (C_u) is set as 1/5, then the frequency scale (C_f) is equal to 80 ($C_f = C_u / C_l$). The models are tested at two wind velocities: U = 8.0 and 14.0 m/s, where U is the mean wind velocity at the top of the building model. Data are collected and recorded for a sampling duration of 163.84 seconds at a sampling rate of 400 Hz, i.e., 65536 data are taken for each channel.

2.2. Aeroelastic model system

The Multi-Degree-of-Freedom (MDOF) aeroelastic model is composed of a seven-story framework for simulating the stiffness, outerwear plates for simulating the geometry shape, and additional weight blocks for simulating the distributions of mass (see Fig. 1). The mass and stiffness of the model are specially designed to be adjustable to some extent.

Its figuration is 0.1 m×0.1 m×0.6 m, the same as the model in the HFFB test. By adjusting the model carefully, the dynamic characteristics of the model are identical in both the along-wind (x) and across-wind (y) directions. The first mode frequency, f_0, of the model is 20.5 Hz, the structural density $\rho_s = 275$ kg/m^3, and the critical structural damping ratio $\zeta = 0.75\%$. The second mode bending frequency of the aeroelastic model is 75 Hz, much higher than its first mode frequency. As a result, the second mode dynamic responses of the model are observed to be much smaller than the first one. Two acceleration sensors are placed at the top of the model to measure the along-wind and across-wind acceleration responses.

The length scale (C_l), velocity scale (C_u) and frequency scale (C_f) are also set as 1/400, 1/5 and 80 respectively. The testing wind velocities, U, are 8.0, 12.0 and 16.0 m/s, i.e., reduced velocities $Ur = U/f_0b$ = 3.9, 5.85 and 7.8 respectively, which cover the normal design wind velocities for tall buildings (Yahyai, *et al*. 1992). Data are recorded for a sampling duration of 120 seconds at a sampling rate of 400 Hz, i.e., 48000 data are taken for each channel.

2.3. Wind field simulation and experimental parameters

Both of the HFFB test and the aeroelastic model test are conducted in the TJ-1 Boundary Layer Wind Tunnel in Tongji University. The working section of the wind tunnel is 18 m long, 1.8 m wide and 1.8 m high; and the wind speed ranges from about 1 m/s to 30 m/s. The biggest blockage in the wind tunnel induced by the principal model and the interfering model is 4%.

Two kinds of 1/400 scale wind models of boundary layer flows, classified as terrain categories B and D in the Chinese load code (GB50009-2001 (2002)), i.e., flows over open terrain and center of large city, are simulated by the combination of turbulence generating spires, a barrier at the entrance of the wind tunnel and roughness elements along the wind tunnel floor upstream of the model. The

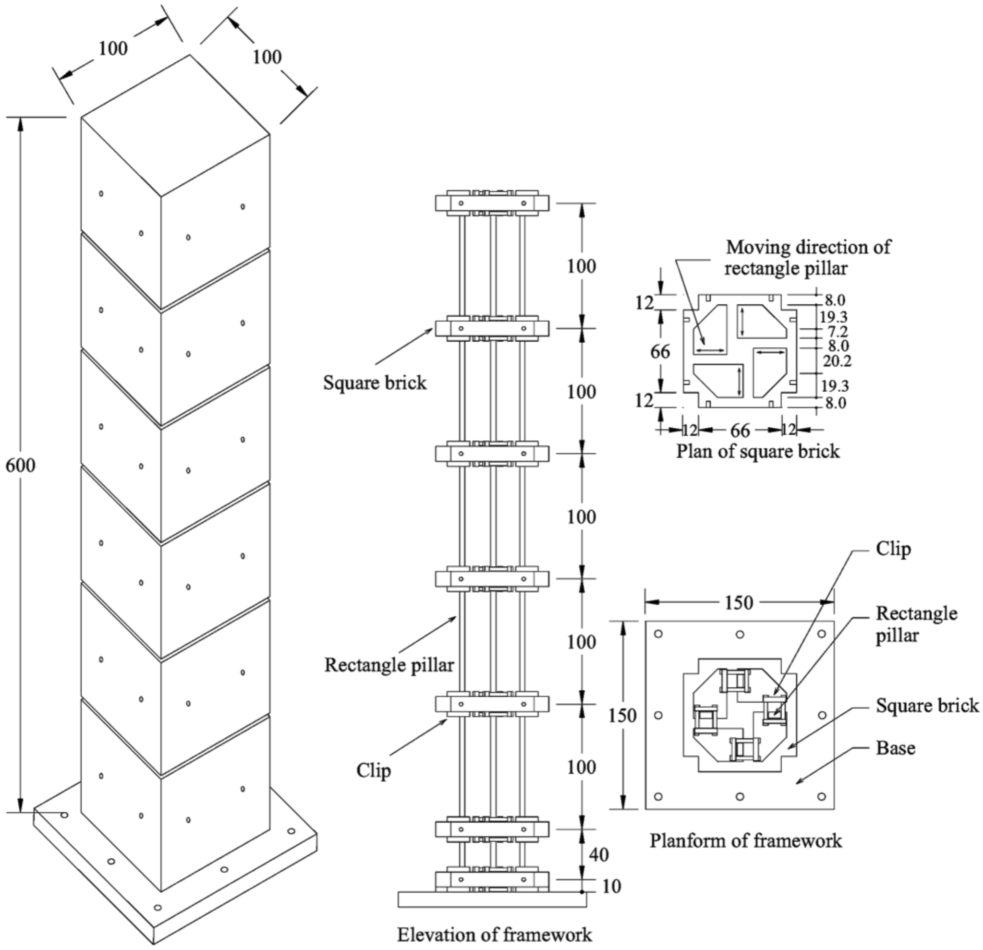

Fig. 1 Aspect and the framework of the Multi-Degree-of-Freedom (MDOF) aeroelastic model (Unit: mm)

flow over Terrain Category B (hereafter referred to as TCB) has a power law exponent of the mean velocity profile $\alpha = 0.16$ and a turbulent intensity at the model height $I_u = 7\%$. The flow over Terrain Category D (hereafter referred to as TCD) has a power law exponent $\alpha = 0.30$ and a turbulent intensity at the model height $I_u = 11.5\%$. The longitudinal integral length scales at 0.50 m high in the wind tunnel are about 0.34 m and 0.23 m for the TCB and TCD flows respectively. Fig. 2 presents the mean wind speed profiles, turbulent intensity profiles and power spectra at the model height of TCB and TCD flows.

In the test, the interfering model is placed at different positions at both upstream and downstream of the principal model. For the interfering model at upstream, the longitudinal space (S_x) between the two models ranges from 0 to 16b, and the lateral space (S_y) ranges from 0 to 4b, where b (=100 mm) is the breadth of the square model. For the interfering model at downstream, S_x ranges from $-1.5b$ to $-3b$, and S_y from 0 to 2.5b. The arrangement of two models is shown in Fig. 3.

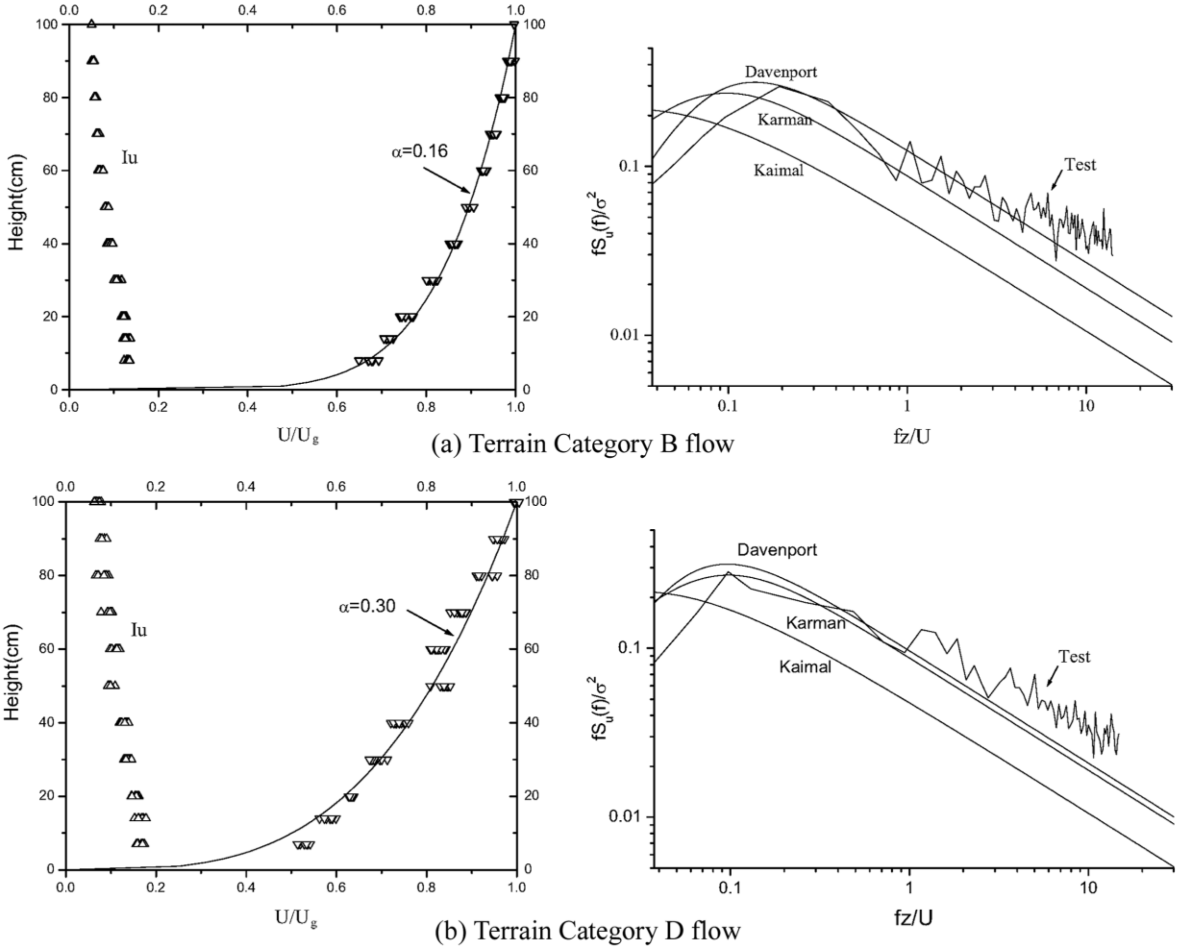

Fig. 2 Mean speed profiles, turbulent intensity profiles and power spectra at the model height of (a) Terrain Category B flow and (b) Terrain Category D flow

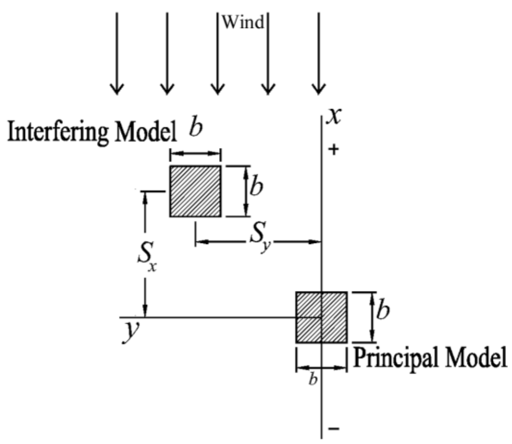

Fig. 3 Arrangement of principal model and interfering model in test

3. Experimental results and discussions

In the HFFB test, the base moment power spectra in along-wind and across-wind directions of the principal model ($S_{Mx}(f)$, $S_{My}(f)$) are measured, which are used to estimate the first mode generalized load power spectra ($S_{Px}(f)$, $S_{Py}(f)$) (with the assumption of linear mode shape):

$$S_P(f) = \frac{S_M(f)}{h^2} \tag{1}$$

where h(= 600 mm) is the height of the model. On the basis of random vibration theory, the first mode response spectrum $S_\xi(f)$ in the generalized coordinate is obtained as following:

$$S_\xi(f) = \frac{1}{k^{*2}}|H(f)|^2 S_P(f) \tag{2}$$

where k^* is the generalized stiffness, and

$$|H(f)|^2 = \frac{1}{\left[1-\left(\frac{f}{f_0}\right)^2\right]^2 + \left(2\zeta\frac{f}{f_0}\right)^2} \tag{3}$$

is the mechanical admittance; ζ is the damping ratio. The RMS value of the displacement at the top of the model is

$$\sigma_T = \left[\int_0^\infty S_\xi(f)df\right]^{\frac{1}{2}} \tag{4}$$

Both the resonance and background components of the responses are included in the RMS displacement.

In the MDOF aeroelastic model test, as the dynamic responses at the top of the model are mainly contributed by the first-mode's response, the RMS value of the displacement at the top of the model (σ_T) is calculated by

$$\sigma_T = \sigma_a/(2\pi f_0)^2 \tag{5}$$

where σ_a is the RMS value of the acceleration response at the top of the model. The acceleration or displacement responses measured on the model include inherently both the background and resonant components.

The along-wind and across-wind dynamic interference factors (IF_{dx} & IF_{dy}) are defined as

$$IF_{dx,dy} = \frac{\text{Along(Across)}-\text{wind RMS displacement at the top of building with interference}}{\text{Along(Across)}-\text{wind RMS displacement at the top of building without interference}} \tag{6}$$

So for the HFFB test, the interference factor IF_{dx} is calculated as (IF_{dy} is the same as IF_{dx}):

$$IF_{dx} = \frac{\sigma_{T_x}}{\sigma^*_{T_x}} = \frac{\left[\int_0^\infty |H(f)|^2 S_{M_x}(f)df\right]^{\frac{1}{2}}}{\left[\int_0^\infty |H(f)|^2 S^*_{M_x}(f)df\right]^{\frac{1}{2}}} \tag{7}$$

where $\sigma^*_{T_x}$ and $S^*_{M_x}(f)$ are the principal model's RMS displacement and the base moment power spectrum without interference in along-wind direction, respectively. It can be found from Eq. (7) that the interference factors are only relevant to the first mode frequency and damping of the principal building and the base moment power spectra, and are independent on the principal buildings stiffness and mass.

3.1. Along-wind dynamic interference effects in TCB

3.1.1. Results from the HFFB test

In the HFFB test, the along-wind fluctuating bending moments of the principal model are measured, then the principal model's dynamic responses and the IF_{dx} values are calculated at $Ur = 3$~9. The critical damping ratio ζ is taken as 0.75% for the principal model with and without interference. As a result, it is found that ζ has little influence on IF_{dx}, that is, the IF_{dx} values vary little with different ζ in the calculation. The IF_{dx} results at $Ur = 5.85$ in TCB are presented in Fig. 4.

When the upstream interfering model locates at $(S_x, S_y) = (2b$~$8b$, 0~$2.5b)$ and $(S_x, S_y) = (12b, 2.5b)$, namely the principal building locates near the edge of the wake of the upstream interfering building, the IF_{dx} values are rather large, the majority of which range from 1.2 to 1.6, with the maximum value of 1.90 at position $(S_x, S_y) = (5b, 1.5b)$ and $Ur = 5.85$.

It is noteworthy that even when the interfering model is placed at far positions, e.g., $(S_x, S_y) = (16b, 2.5b)$, the IF_{dx} values still range from 1.15 to 1.25 at $Ur = 3$~9, which means that the dynamic interference effects still exist when two building's space is rather far. This result is consistence with that of Reference (Saunders and Melbourne 1980).

When the interfering model locates at the downstream of the principal model, the dynamic interference factors are usually less than 1 in most cases. But at downstream position $(S_x, S_y) = (-1.5b, 1.5b)$, $IF_{dx} = 1.73$ at $Ur = 5.85$.

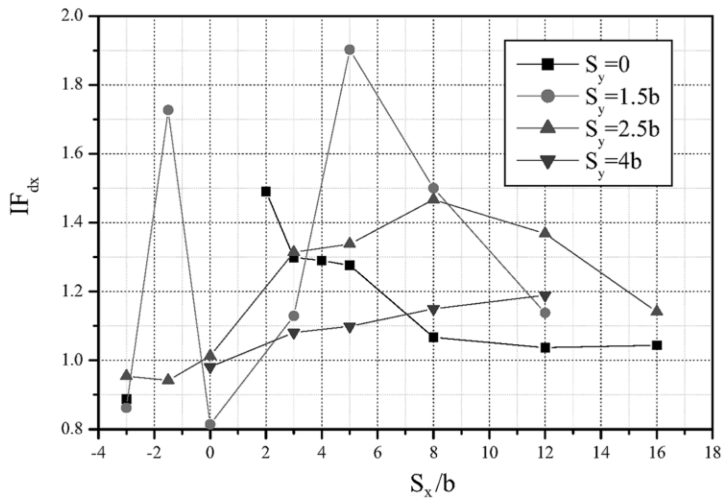

Fig. 4 IF_{dx} values from the high-frequency-force-balance test at $Ur = 5.85$ in Terrain Category B

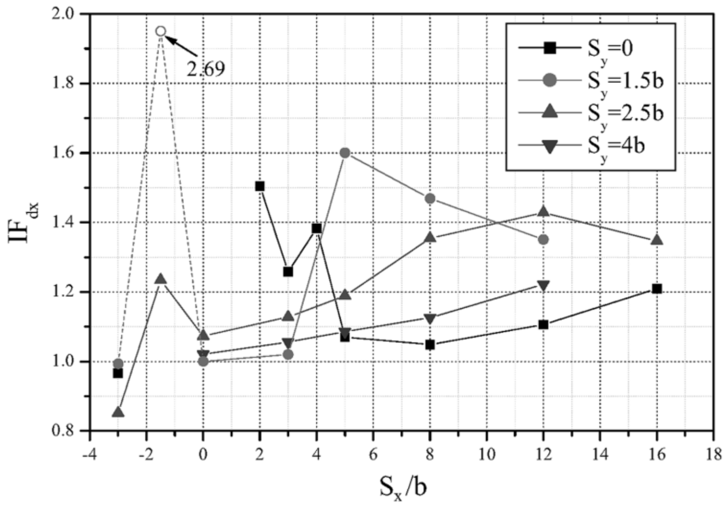

Fig. 5 IF_{dx} values from the aeroelastic model test at Ur = 5.85 in Terrain Category B

3.1.2. Results from the aeroelastic model test

In the aeroelastic model test, the models are tested at Ur = 3.9, 5.85 and 7.8. Fig. 5 indicates the IF_{dx} values in TCB at Ur = 5.85. The results from the two kinds of tests have common tendency. When the interfering model locates at $(S_x, S_y) = (2b\sim12b, 0\sim2.5b)$, the IF_{dx} values from the aeroelastic model test are rather large, the majority of which range from 1.2 to 1.6. The maximum value of IF_{dx} is 1.99 at position $(S_x, S_y) = (2b, 0)$ and Ur = 3.9, while the corresponding value from the HFFB test at same configuration is 1.84. For Ur = 5.85, the maximum IF_{dx} values from the two kinds of tests both happens at position $(S_x, S_y) = (5b, 1.5b)$, with the values 1.60 for the aeroelastic model test and 1.90 for the HFFB test. The difference of the results between two tests may be owed to the variation of aerodynamic damping of the principal aeroelastic model before and after being interfered, which can not be reflected in the HFFB test. The effects of aerodynamic damping are discussed in detail in Huang and Gu (2003). By considering the effects of aerodynamic damping, the results from the two kinds of tests are closer.

When the interfering model locates at the downstream, the dynamic interference factors are usually close to 1 in most cases. But at downstream position $(S_x, S_y) = (-1.5b, 1.5b)$, IF_{dx} is 2.69 (at Ur = 5.85) and 1.64 (at Ur = 7.8) in TCB. There are similar results in Reference (Bailey and Kwok 1985), in which IF_{dx} is 4.36 at position $(S_x, S_y) = (-1.5b, 1.22b)$ and Ur = 6 and in open terrain flow field. In these critical cases, a wind channel is produced between the two models, and the airflow converges and accelerates in the channel, which results in the high dynamic response of the principal model.

3.2. Across-wind dynamic interference effects in TCB

3.2.1. Results from the HFFB test

The across-wind interference factors IF_{dy} are also calculated at Ur = 3~9 and critical damping ratio ξ of 0.75%. Similarly, it is found that ζ has little influence on IF_{dy}. Fig. 6 shows the IF_{dy} results at Ur = 5.85 in TCB.

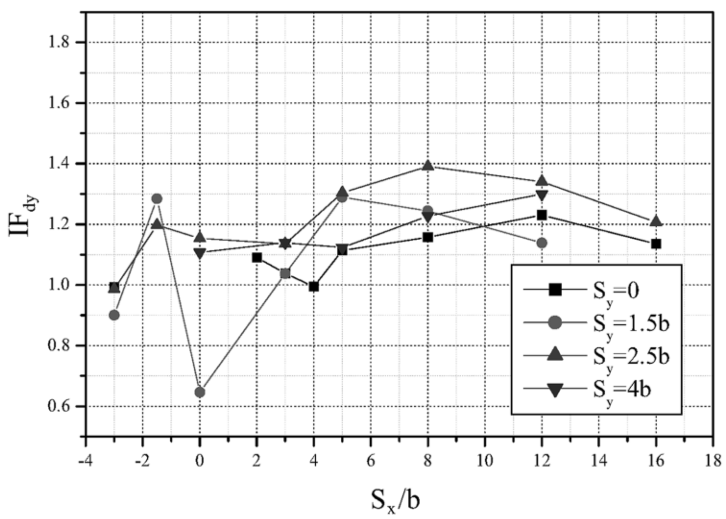

Fig. 6 IF_{dy} values from the high-frequency-force-balance test at Ur = 5.85 in Terrain Category B

When the principal model locates near the edge of the wake of the upstream interfering building, the IF_{dy} values range from 1.1 to 1.5. When the interfering model locates at the downstream of the principal model, the interference effects are not significant for most cases. But when two models are arranged side by side, e.g., $(S_x, S_y) = (0, 2.5b)$, the IF_{dy} value is large up to 1.84 at Ur = 7.8.

3.2.2. Results from the aeroelastic model test

IF_{dy} values from the aeroelastic model test at Ur = 5.85 in TCB are presented in Fig. 7. When the interfering model locates at $(S_x, S_y) = (5b\sim12b, 2.5b\sim4b)$, the IF_{dy} values are in the scope of 1.1 to

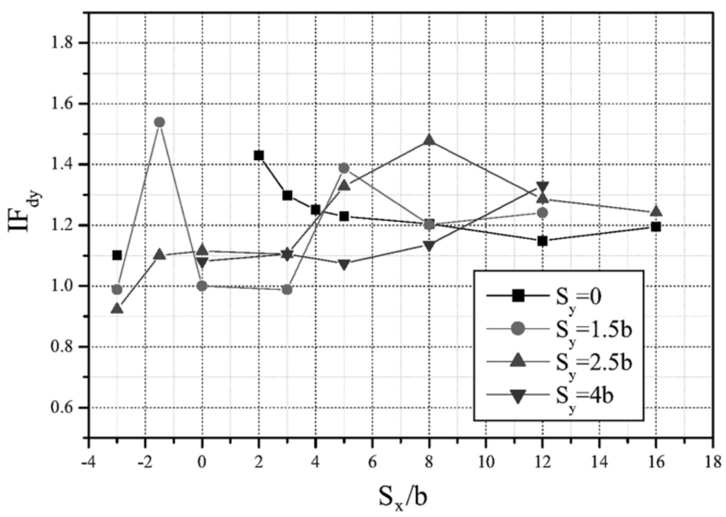

Fig. 7 IF_{dy} values from the aeroelastic model test at Ur = 5.85 in Terrain Category B

1.5. Similarly to the results from the HFFB test, when interfering model locates at $(S_x, S_y) = (0, 2.5b)$, IF_{dy} is large up to 1.63 at $Ur = 7.8$. But when the interfering model locates at $(S_x, S_y) = (2b, 0)$ and $(5b, 0)$, the IF_{dy} values are 1.78 and 1.68 at $Ur = 3.9$, respectively. The corresponding values from the HFFB test are only 1.35 and 1.20, respectively. This difference and other above-mentioned differences of interference factors from the two kinds of tests may also be owed to the effects of the aerodynamic damping (Huang and Gu 2003).

3.3. Results in TCD and the influence of turbulence intensity

Maximum interference effects can be expected for the open terrain exposure, steadily reducing for

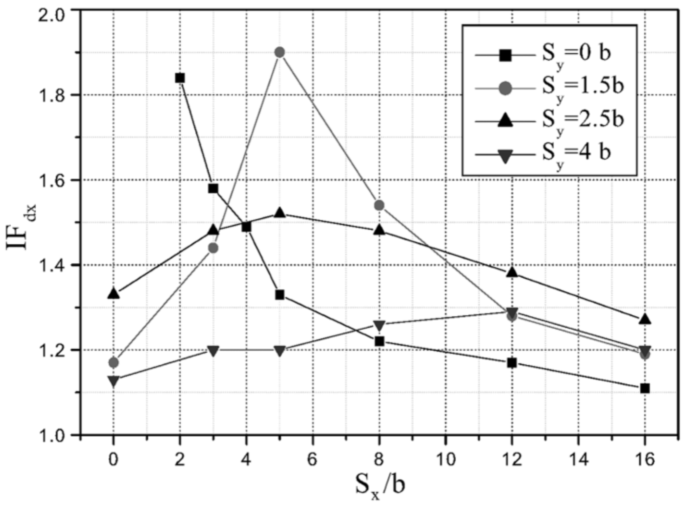

(a) IF_{dx}

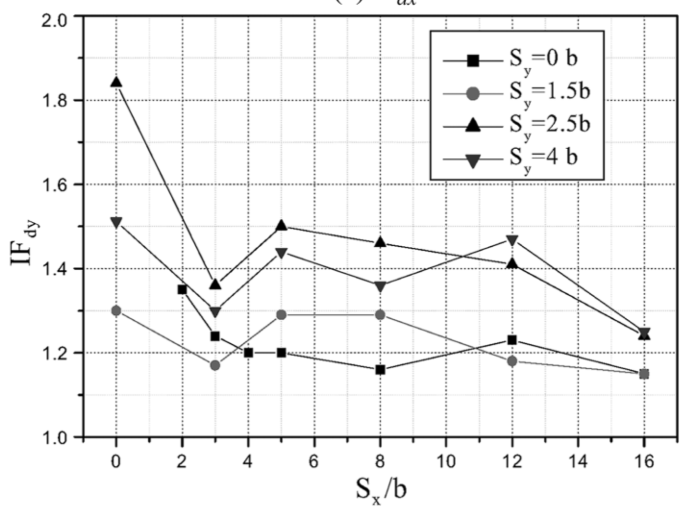

(b) IF_{dy}

Fig. 8 Maximum values of dynamic interference factors from the high-frequency-force-balance test at Ur = 3~9 in Terrain Category B the suburban and reaching a minimum for the urban terrain (Khanduri, *et al*. 1998). Comparing with the interference factors in TCB, it is found that the interference factors in TCD, IF_{dx} and IF_{dy}, decrease in general to some extent,

When the upstream interfering model locates at $(S_x, S_y) = (2b\sim8b, 0\sim2.5b)$, the IF_{dx} values in TCD are relatively large, the majority of which range from 1.1 to 1.4. The maximum IF_{dx} from the HFFB test is 1.57 at position $(S_x, S_y) = (5b, 1.5b)$ and $Ur = 5.85$, and the one from the aeroelastic model test is 1.47 at position $(S_x, S_y) = (8b, 2.5b)$ and $Ur = 3.9$.

In the across-wind direction, the IF_{dy} values in TCD are relatively large when the upstream interfering model locates at $(S_x, S_y) = (3b\sim8b, 2.5b\sim4b)$, the majority of which range from 1.1 to 1.4. But when two models are arranged side by side ($(S_x, S_y) = (0, 2.5b)$), IF_{dy} is large up to 1.61 for the HFFB test and 1.62 for the aeroelastic model test at $Ur = 7.8$, respectively.

By analyzing the interference factors from the present study and other Saunders and Melbourne (1980), Blessmann (1985), Bailey and Kwok (1985), Kwok (1989), Kareem (1987), Taniike and Inaoka (1988) and Taniike (1991), it is found that the influence of the upstream terrain is mainly contributed by the turbulence intensity in the flow field, while the profile of mean wind speed has little influence.

Fig. 8 shows the maximum values of IF_{dx} and IF_{dy} from the HFFB test in TCB at $Ur = 3\sim9$. The results from the HFFB test are independent on the principal model's mass, stiffness and damping, as mentioned above. In order to illustrate the effects of turbulence intensity on the interference factors, two ratios between IF_{dx} and IF_{dy} in different wind fields from the References, Saunders and Melbourne (1980), Blessmann (1985), Bailey and Kwok (1985), Kwok (1989), Kareem (1987) and Taniike and Inaoka (1988) and the corresponding factors in TCB from the present study are defined as R_x and R_y respectively, i.e.,

$$R_x(R_y) = \frac{\begin{array}{c} IF_{dx}\ (IF_{dy}) \text{ in different wind fields from the References (Saunders and Melbourne 1980, Blessmann} \\ \text{1985, Bailey and Kwok 1985, Kwok 1989, Kareem 1987, Taniike and Inaoka 1988)} \end{array}}{IF_{dx}\ (IF_{dy}) \text{ in TCB from the present study}} \tag{8}$$

The ratios are listed in Table 2. From this table it can be found that the IF_{dx} and IF_{dy} values decrease rapidly with the increase of turbulence intensities. This is similar to the conclusion given by Taniike (1991).

Table 2 Mean ratios of IF_{dx} and IF_{dy} in different flow fields to this paper's values in TCB

I_u at 2/3 height of model	$I_u < 8\%$	$8\% \le I_u < 12\%$	$12\% \le I_u < 14\%$	$14\% \le I_u < 16\%$	$I_u \ge 16\%$
Relevant literatures	Refs. (Kareem 1987, Taniike and Inaoka 1988)	This study in TCB and Refs. (Saunders and Melbourne 1980, Bailey and Kwok 1985)	This study in TCD	Ref. (Kwok 1989)	Refs. (Blessmann 1985, Kwok 1989, Taniike and Inaoka 1988)
R_x	About 2.0	1.0	0.92	0.84	About 0.7 and $IF_{dx} \ge 1.0$
R_y	About 2.0	1.0	0.95	0.90	0.85

4. Generalization using neural networks and recommendations for wind load codes

Because there are too many parameters involved in the study of interference effects, it is impossible to test all configurations in the wind tunnel. Thus the artificial neural networks (ANN) method, an offshoot of the research in the field of artificial intelligence (AI), is used in this study to generalize the limited experimental data. Two small Back-Propagation Neural Networks (BPNN) systems are developed to simulate the along-wind and across-wind dynamic interference effects (IF_{dx} and IF_{dy}). As a result, some new IF_{dx} (and IF_{dy}) values for the untested configurations are proposed according to the trained BPNN system.

The simulating process of IF_{dx} is presented in the following as an example. The BPNN system adopts a three-layer network structure, which includes one input layer, one hidden layer and one output layer. The input layer has two input neurons (or nodes), which represent the longitudinal and

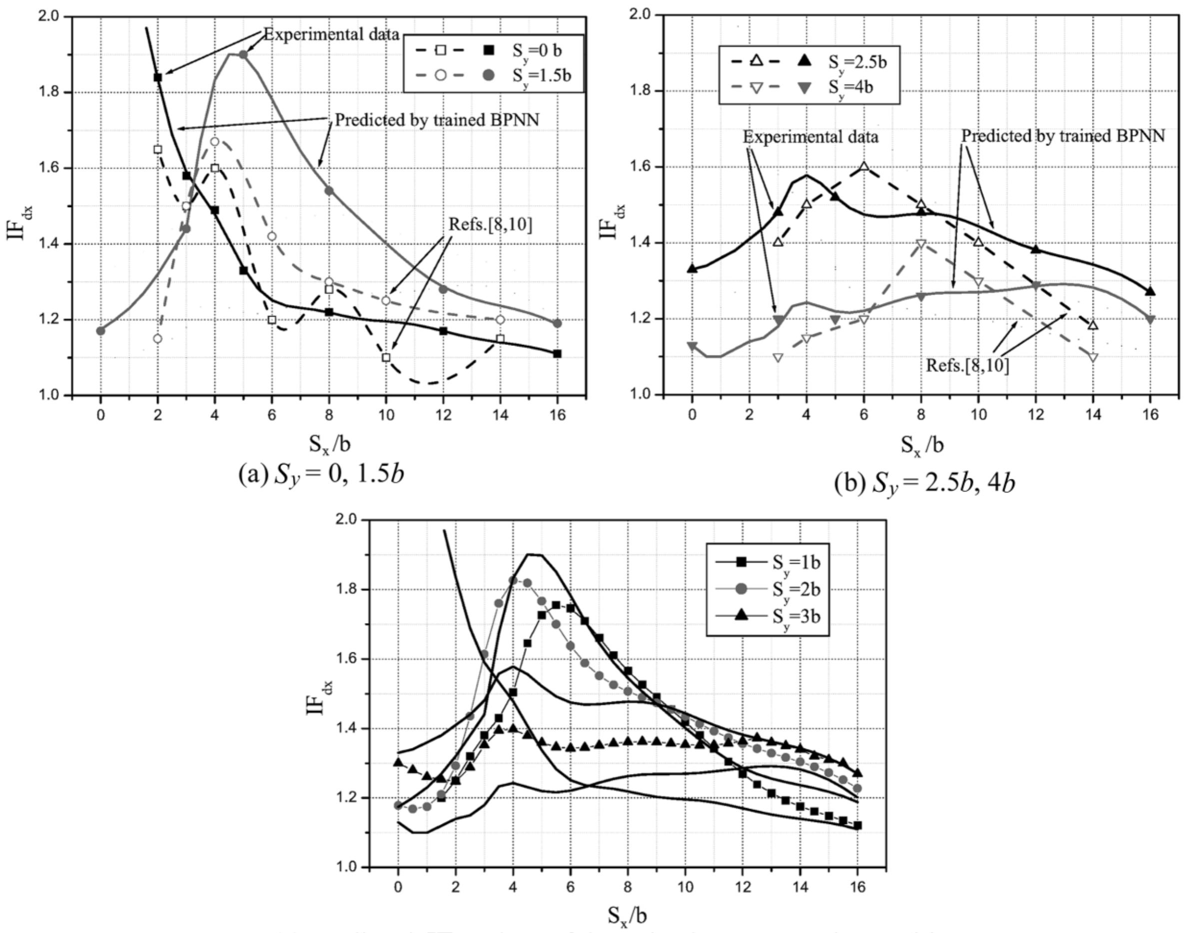

(a) $S_y = 0$, $1.5b$

(b) $S_y = 2.5b$, $4b$

(c) Predicted IF_{dx} values of the trained BPNN at other positions

Fig. 9 Comparison of predicted IF_{dx} values of the trained BPNN with data of Saunders and Melbourne (1980), Bailey and Kwok (1985) lateral space between two buildings (S_x/b and S_y/b). The hidden layer has 15 neurons, while the output layer has only one neuron, which represents the IF_{dx} value for the corresponding case. The maximum values of IF_{dx} from the HFFB test at Ur = 3~9 in TCB (see Fig. 8(a)) are selected as the training data of the BPNN system, which are also presented in Figs. 9(a) and 9(b) (scattered solid symbol). The learning process is repeated until the error between the actual and desired outputs are small enough to satisfy a user-defined threshold.

In order to verify the applicability of the well-trained BPNN system, the BPNN system is tested using new experimental data from Saunders & Melbourne (1980) and Bailey & Kwok (1985), in which the flow fields are similar to the TCB flow in this study (see Table 2). The comparison between the new experimental data in Saunders & Melbourne (1980), Bailey & Kwok (1985) and the predicted IF_{dx} values of the trained BPNN (solid line) are shown in Figs. 9(a) and 9(b). Although there are some differences in the configurations between these tests (such as that Ur = 2, 4, 6 in Saunders & Melbourne (1980) and Ur = 6 in Bailey & Kwok (1985), the predicted IF_{dx} values of the trained BPNN coincide with the experimental data Saunders and Melbourne (1980), Bailey and Kwok (1985) in general.

When the interfering building locates at other positions, the IF_{dx} values are obtained according to the trained BPNN. The predicted IF_{dx} values are shown in Fig. 9(c). It can be seen that the suggested values are in the reasonable range. Based on the IF_{dx} values in positions range (S_x, S_y) = (0~16b, 0~4b) and referring to other papers, the IF_{dx} contour map is finally obtained as shown in Fig. 10(a). IF_{dx} reaches the maximum value 1.90 at the position (S_x, S_y) = (5b, 1.5b) and decreases gradually along with the increase of the distance to this critical position. For the far positions (S_x = 16b),

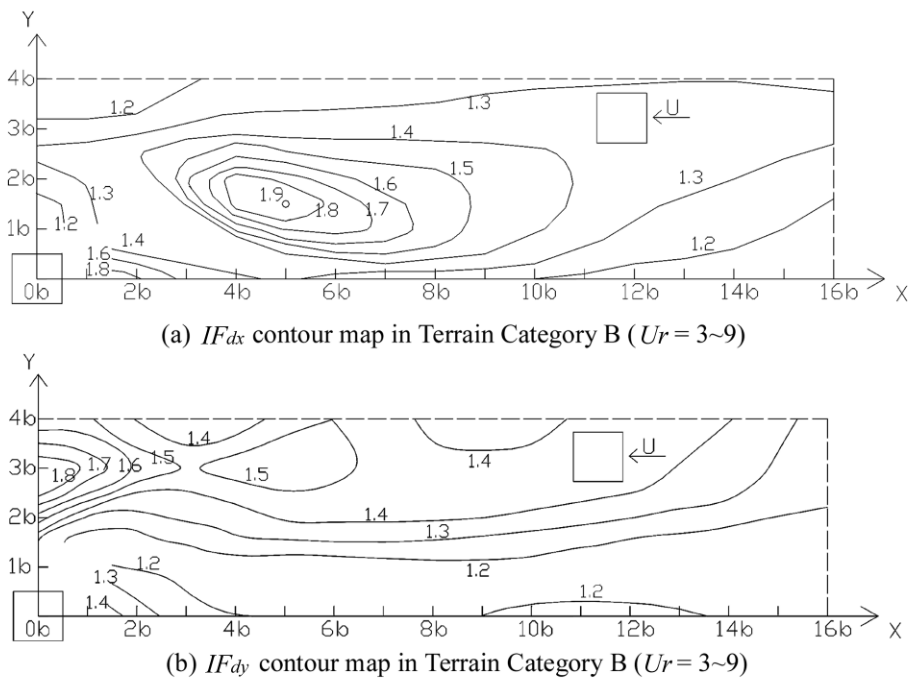

Fig. 10 (a) IF_{dx} contour map in Terrain Category B (Ur = 3~9), (b) IF_{dy} contour map in Terrain Category B (Ur = 3~9) the IF_{dx} values are still rather large, which may equal to 1.3.

By using the same method, the IF_{dy} contour map is also obtained, which is presented in Fig. 10b. For the across-wind direction, the IF_{dy} values are relatively small when the interfering model locates at the upstream of the principal model. But for the side-by-side positions, (S_x, S_y) = (0~0.5b, 2.5b~3.2b), the IF_{dy} values are large up to 1.8.

5. Conclusions

In this paper, the interference effects on dynamic response between two identical tall building models with square cross-sections are experimentally studied by using high-frequency-force-balance technique. Another wind tunnel test on two building models, in which the principal model is an aeroelastic one, is also carried out to further study the interference effects, which verifies the results from the HFFB test.

According to the HFFB test, When the upstream interfering model locates at $(S_x, S_y) = (2b\sim8b$, 0~2.5b), namely the principal model locates near the edge of the wake of the upstream interfering model, the IF_{dx} and IF_{dy} values are rather large, the majority of which range from 1.2 to 1.6 in open terrain, with the maximum value of 1.9. When the interfering model locates at the downstream or side-by-side positions of the principal model, the interference effects are usually inapparent for most cases, but the IF_{dx} and IF_{dy} values may be up to 1.7~1.8 at few special configurations. The results from the aeroelastic model test have common tendency.

The artificial neural networks method is used to deal with the experimental data. Two BPNN Systems are developed to simulate the along-wind and across-wind dynamic interference effects. The IF_{dx} and IF_{dy} contour maps are finally obtained, which may be used as references for wind load codes.

Acknowledgements

This research is jointly supported by the National Science Foundation (50321003), the Foundation for University Key Teachers by the Ministry of Education of China. Their supports are gratefully acknowledged.

References

Bailey, P.A. and Kwok, K.C.S. (1985), "Interference excitation of twin tall buildings", *J. Wind Eng. Ind. Aerodyn.*, **21**, 323-338.

Blessmann, J. (1985), "Buffeting effects on neighbouring tall buildings", *J. Wind Eng. Ind. Aerodyn.*, **18**, 105-110.

Chinese Code for Loading on Buildings and Structures, GB50009-2001, (2002), Architectural Industry Press of China, Beijing.

Huang, P. and Gu, M. (2003), "Experimental study on aerodynamic damping of tall building after being interfered", *Journal of Tongji University*, **31**(6), 652-656 (in Chinese)

Kareem, A. (1987), "The effect of aerodynamic interference on the dynamic response of prismatic structures", *J. Wind Eng. Ind. Aerodyn.*, **25**, 365-372.

Khanduri, A.C. (2000), "Generalization of wind-induced interference effects for two buildings", *Wind and Struct., An Int. J.*, **3**(4), 255-266.

Khanduri, A.C., Stathopoulos, T. and Bedard, C. (1998), "Wind-induced interference effects on buildings - a review of the state-of-the-art", *Eng. Struct.*, **20**(7), 617-630.

Kwok, K.C.S. (1989), "Interference effects on tall buildings", *Proceedings of 2nd Asia-pacific Symposium on Wind Engineering*, Beijing, China, June, **1**, 446-453.

Kwok, K.C.S. (1995), "Aerodynamics of the tall buildings", *A State of the Art in Wind Engineering, Ninth International Conference on Wind Engineering*, New Delhi, India, 180-204.

Sakamoto, H., Haniu, H. and Obata, Y. (1987), "Fluctuating forces acting on two square prisms in a tandem arrangement", *J. Wind Eng. Ind. Aerodyn*., **26**, 85-103.

Saunders, J.W. and Melbourne, W.H. (1980), "Buffeting effects of upstream buildings", J.E. Cermak (Ed.), *Proc. 5th Int. Conf. on Wind Engineering, Fort Collins, CO, 1979*, Pergamon, Oxford, **1**, 593-606.

Taniike, Y. (1991), "Turbulence effect on mutual interference on tall buildings", *J. Eng. Mech.*, ASCE, **117**(3), 443-456.

Taniike, Y. (1992), "Interference mechanism for enhanced wind forces on neighbouring tall buildings", *J. Wind Eng. Ind. Aerodyn*., **41-44**, 1073-1083.

Taniike, Y. and Inaoka, H. (1988), "Aeroelastic behavior of tall buildings in wakes", *J. Wind Eng. Ind. Aerodyn*., **28**, 317-327.

Thepmongkorn, S., Wood, G.S. and Kwok, K.C.S. (2002), "Interference effects on wind-induced coupled motion of a tall building", *J. Wind Eng. Ind. Aerodyn*., **90**, 1807-1815.

Thoroddsen, S.T., Cermak, J.E. and Peterka, J.A. (1985), "Mean and dynamic wind loading caused by an upwind structure", *Proceedings of 5th U.S. National Conference on Wind Engineering*, Lubboch, USA, November, 4A-73~4A-80.

Yahyai, M., Kumar, K., Krishna, P. and Pande, P.K. (1992), "Aerodynamic interference in tall rectangular buildings", *J. Wind Eng. Ind. Aerodyn*., **41-44**, 859-866.

CC